Using a Modified Soil-Plant-Atmosphere Scheme (MSPAS) to Simulate the Interaction between Land Surface Processes and Atmospheric Boundary Layer in Semi-Arid Regions

LIU Shuhua[1,2] (刘树华), YUE Xu[1] (乐 旭), HU Fei[2] (胡 非), and LIU Huizhi[2] (刘辉志)

[1]*Group of Atmosphere Boundary Layer and Turbulence, Laboratory of Severe Storm Research, Department of Atmospheric Sciences, the College of Physics, Peking University, Beijing* 100871

[2]*State Key Laboratory of Atmospheric Physics and Chemistry, Institute of Atmospheric Physics, Chinese Academy of Sciences, Beijing* 100029

(Received 8 May 2002; revised 3 September 2003)

ABSTRACT

This paper uses a Modified Soil-Plant-Atmosphere Scheme (MSPAS) to study the interaction between land surface and atmospheric boundary layer processes. The scheme is composed of two main parts: atmospheric boundary layer processes and land surface processes. Compared with SiB and BATS, which are famous for their detailed parameterizations of physical variables, this simplified model is more convenient and saves much more computation time. Though simple, the feasibility of the model is well proved in this paper. The numerical simulation results from MSPAS show good agreement with reality. The scheme is used to obtain reasonable simulations for diurnal variations of heat balance, potential temperature of boundary layer, and wind field, and spatial distributions of temperature, specific humidity, vertical velocity, turbulence kinetic energy, and turbulence exchange coefficient over desert and oasis. In addition, MSPAS is used to simulate the interaction between desert and oasis at night, and again it obtains reasonable results. This indicates that MSPAS can be used to study the interaction between land surface processes and the atmospheric boundary layer over various underlying surfaces and can be extended for regional climate and numerical weather prediction study.

Key words: modified soil-plant-atmosphere scheme (MSPAS), land surface processes (LSP), atmospheric boundary layer

1. Introduction

As a part of general circulation models (GCMs), the study of land surface processes has become a most challenging work, which attracts more and more researchers' attention. Physical conditions of the continent surface, such as soil moisture, vegetation coverage, vegetation leaf area index, and reflectivity, can directly affect mass exchanges and energy exchanges between the surface layer and atmosphere, and then consequently affect the structure of the atmospheric boundary layer, the atmospheric circulation, and regional climate. Therefore, in both climate models and atmospheric boundary layer models, their effects should be considered. In the research on models of micro-mesoscale climate and the atmosphere boundary layer over different underlying surfaces, they are especially important. Mass exchanges and the energy exchanges between soil, vegetation, and the atmosphere, and interaction processes between the earth and the atmosphere are immensely important for the development of the boundary layer. In particular, radiation fluxes, momentum fluxes, sensible heat fluxes, and latent heat fluxes affect the movement of the atmosphere and the fields of temperature, moisture, and precipitation, which then have strong feedback functions on the source and congruence of these physical quantities. The transferring of energy and mass between land surface and atmosphere is an important subject in the studies of soil-vegetation-atmosphere interactions in scale micro and mesoscale atmospheric processes. The atmospheric processes in the boundary layer (lower

*E-mail: Lshuhua@pku.edu.cn

layer atmosphere) at the border region between desert and oasis are closely related to the climatic variation, ecological equilibrium, and agricultural development in the semi-arid regions.

Models for land surface processes have been developed for more than 20 years. Bhumralkar (1975) and Blackadar (1976) proposed a 12-layer model for the prediction of ground surface temperature, which gave good results against observations. Charney et al. (1977) studied the influence of the variation of surface reflective index on climate. They found that it had an important influence on the climate in arid areas. Mahfouf et al. (1987) studied the influences of soil and vegetation on the development of mesoscale circulation.

As a milestone, Deardorff's (1978) research work proved that sound results could be obtained by simple simulations. In his paper, he compared five approximate methods in predicting ground surface temperature with the 12-layer soil model, and concluded that the forcing restore method was the most plausible one. Analogously, he utilized the same method in the prediction of soil water content, and got reasonable results as expected. In this paper, we adopt his parameterization methods in the land surface part of our scheme.

Noilhan and Planton (1989) proposed a most effective simulation method of their time. They continued to use the same way as Deardorff did in predicting ground surface temperature and soil moisture content. However, they made great improvements in the parameterization of vegetation, which enhanced the accuracy in calculating specific humidity on the ground and made the computation more physically reasonable. The feasibility of this model has been approved by Sang et al. (1992) and Liu et al. (2002).

In the 1980s, two important models (BATS, Dickinson et al., 1986, 1993; and SiB, Sellers et al., 1986, 1996) were developed. And from then on, the simulations of land surface processes (LSP) have been improving continuously and many models are built with various complexities.

In this paper, we attempt to develop a Modified Soil-Plant-Atmosphere Scheme (MSPAS) to simulate land surface and boundary layer processes in the semi-arid region. We mainly utilize the methods proposed by Deardorff (1978) in the land surface parameterization, combined with the revisions made by Noilhan and Planton (1989), which make our model more physically plausible.

Compared with SiB and BATS, which are detailed in the variables' parameterization, our model is somewhat simple. However, the feasibility of this model has been well proved in this paper. As you will find, the model reasonably describes many common phenomena in semi-arid regions, for example, we simulate moisture inversion on the desert close to oasis, and this phenomenon has been observed by Hu et al. (1993) and also well predicted by Liu et al. (1997). In our next paper, some sensitivity experiments are designed to test the stability and sensibility of MSPAS. All the work proves that MSPAS can be used to study the interaction between land surface processes and the atmospheric boundary layer over various underlying surfaces and that it is suitable for further studies associated with desertification and reforestation in China.

2. Numerical model and parameterization

2.1 *Basic equations*

The model considers a two-dimensional spatial distribution, because in the condition that the ground is smooth and regular, we can make the assumption that the movement of atmosphere is uniform horizontally. So the two-dimensional momentum, thermodynamic, water vapor, continuity, and static equilibrium equations can be written as (e.g., Stull, 1991 or Liu and Liu, 1991),

$$\frac{\partial u}{\partial t} = -u\frac{\partial u}{\partial x} - w\frac{\partial u}{\partial z} - \theta\frac{\partial \pi}{\partial x} + K_{\mathrm{H}}\frac{\partial^2 u}{\partial x^2} + \frac{\partial}{\partial z}(K_m\frac{\partial u}{\partial z})\,, \tag{1}$$

$$\frac{\partial \theta}{\partial t} = -u\frac{\partial \theta}{\partial x} - w\frac{\partial \theta}{\partial z} + K_{\mathrm{H}}\frac{\partial^2 \theta}{\partial x^2} + \frac{\partial}{\partial z}(K_\theta\frac{\partial \theta}{\partial z})\,, \tag{2}$$

$$\frac{\partial q}{\partial t} = -u\frac{\partial q}{\partial x} - w\frac{\partial q}{\partial z} + K_{\mathrm{H}}\frac{\partial^2 q}{\partial x^2} + \frac{\partial}{\partial z}(K_q\frac{\partial q}{\partial z})\,, \tag{3}$$

$$\frac{\partial w}{\partial z} + \frac{\partial u}{\partial x} = 0\,, \tag{4}$$

$$\frac{\partial \pi}{\partial z} = -\frac{g}{\theta}\,, \tag{5}$$

where x and z denote the horizontal and vertical coordinates respectively, and u and w (m s^{-1}) are the velocities in the corresponding directions.

$$\pi = c_p\left(\frac{p}{p_0}\right)^{0.286}$$

is the Exner function. K_{H} is the horizontal eddy coefficient, whose value is set to 10.0 in the model. K_m, K_θ, K_q, and K_{e^2} are the vertical coefficients for momentum, temperature, humidity, and turbulence kinetic energy. The relations among them are that: $K_\theta = K_q = 1.35K_m$ and $K_m = K_{e^2}$. We only need to figure out one of the values so as to get the others (see 2.2). Other symbols are listed in the appendix of this paper.

2.2 *Turbulence parameterization*

The energy closed method is used in the solution of the model. According to the empirical formula given

by Yamada (1983),

$$\frac{\partial e^2}{\partial t} = -u\frac{\partial e^2}{\partial x} - w\frac{\partial e^2}{\partial z} + K_{\rm H}\frac{\partial^2 e^2}{\partial x^2} + \frac{\partial}{\partial z}(K_{e^2}\frac{\partial e^2}{\partial z}) + K_m\left(\frac{\partial u}{\partial z}\right)^2 - K_\theta\frac{g}{\theta}\frac{\partial\theta}{\partial z} - \frac{B_1 e^3}{L}\,, \tag{6}$$

where

$$e^2 = \frac{1}{2}(\overline{u'^2} + \overline{w'^2})$$

is the kinetic energy of turbulence. $B_1 e^3/L$ is the dissipation of energy with an empirical constant B_1, which is set to 0.25 here. L is the master turbulence length scale, and its value can be obtained as follows:

$$L = \frac{kz}{\left(1 + \dfrac{kz}{L_\infty}\right)} \tag{7}$$

with

$$L_\infty = 0.1\frac{\int_0^\infty e^2 z dz}{\int_0^\infty e^2 dz}\,, \tag{8}$$

where k is the von Kármán constant. And we can calculate K_m from

$$K_m = 0.5L(e^2)^{1/2}\,. \tag{9}$$

2.3 *Parameterization of land surface*

2.3.1 *Energy budget between land surface and atmosphere*

As the external force, energy from the sun causes all the movement of the atmosphere and also determines the physical conditions of land, such as temperature, humidity, and so on. In this paper, we intend to discuss the correlation between the air above desert and oasis, so the fraction of vegetation needs to be considered. We take the air just above the canopy ($z = z_{\rm a}$) as the reference layer, and then the energy balance equation is (Deardorff, 1978):

$$S_{\rm h}^{\downarrow} + R_{\rm Lh}^{\downarrow} - S_{\rm h}^{\uparrow} - R_{\rm Lh}^{\uparrow} - (S_{\rm g}^{\downarrow} + R_{\rm Lg}^{\downarrow} - S_{\rm g}^{\uparrow} - R_{\rm Lg}^{\uparrow}) = H_{\rm sh} - H_{\rm sg} + L_{\rm v}(E_{\rm h} - E_{\rm g}) \tag{10}$$

where S and $R_{\rm L}$, are the shortwave and longwave radiation flux, respectively. H is the sensible heat flux and $L_{\rm v}E$ is the latent heat flux of vapor. $L_{\rm v}$ is the latent heat rate of water vapor. Subscript g means the value on the ground while subscript h denotes the value at the height of $z = z_{\rm a}$. The arrows denote the direction of radiation: $\uparrow$ means upwards and $\downarrow$ means downwards. On the left side of (10), $S_{\rm h}^{\downarrow}$ and $R_{\rm Lh}^{\downarrow}$ are assumed known,

$$S_{\rm h}^{\downarrow} = (1 - 0.8\sigma_{\rm c})\cdot(1-\alpha)S_0\sin h\,, \tag{11}$$

$$R_{\rm Lh}^{\downarrow} = [\sigma_{\rm c} + (1-\sigma_{\rm c})0.67(1670q_{\rm a})^{0.08}]\sigma T_{\rm a}^4\,, \tag{12}$$

"$\sin h$" is the azimuth of the sun, which can be obtained from Wang (1987):

$$\sin h = \sin\varphi\cdot\sin\delta + \cos\varphi\cdot\cos\delta\cdot\cos\omega\,, \tag{13}$$

and then by the definition of $\sigma_{\rm f}, \varepsilon_{\rm g}, \varepsilon_{\rm f}, \alpha_{\rm g}, \alpha_{\rm f}, \alpha$, we can obtain all the other radiation terms (Deardorff, 1978).

As for the right side of the equation, we define that

$$H_{\rm sf} = H_{\rm sh} - H_{\rm sg}\,, \tag{14a}$$

and

$$E_{\rm f} = E_{\rm h} - E_{\rm g}\,, \tag{14b}$$

so equation (10) can be extended as:

$$\sigma_{\rm f}[(1-\alpha_{\rm f})S_{\rm h}^{\downarrow} + \varepsilon_{\rm f}R_{\rm Lh}^{\downarrow} + \frac{\varepsilon_{\rm f}\varepsilon_{\rm g}}{\varepsilon_{\rm f}+\varepsilon_{\rm g}-\varepsilon_{\rm f}\varepsilon_{\rm g}}\sigma T_{\rm g}^4 - \frac{(\varepsilon_{\rm f}+2\varepsilon_{\rm g}-\varepsilon_{\rm f}\varepsilon_{\rm g})}{(\varepsilon_{\rm f}+\varepsilon_{\rm g}-\varepsilon_{\rm f}\varepsilon_{\rm g})}\varepsilon_{\rm f}\sigma T_{\rm f}^4] = H_{\rm sf} + L_{\rm v}E_{\rm f}\,, \tag{15}$$

where subscript f means the properties on the surface of the foliage and $\alpha_{\rm f} = 0.20$ is the vegetable albedo, while $\alpha_{\rm g}$ is the ground albedo:

$$\begin{cases} \alpha_{\rm g} = 0.31 - 0.17w_{\rm g}/w_{\rm k} & (w_{\rm g} \leqslant w_{\rm k})\,, \\ \alpha_{\rm g} = 0.14 & (w_{\rm g} > w_{\rm k})\,, \end{cases} \tag{16}$$

where parameters $w_{\rm g}$ and $w_{\rm k}$ are the water fraction in the soil (see 2.3.2). Equation (15) is used to solve $T_{\rm f}$ by the Newton-Raphson method.

The energy balance of the ground is

$$-G = H_{\rm sg} + L_{\rm v}\cdot E_{\rm g} - (1-\alpha_{\rm g})S_{\rm g}^{\downarrow} + R_{\rm Lg}^{\uparrow} - R_{\rm Lg}^{\downarrow}\,, \tag{17}$$

where G is the soil heat flux.

In order to figure out the values of $T_{\rm f}$ and G, we need to get the values of H and E first. For bare ground,

$$E_{\rm h} = E_{\rm g} = \rho_{\rm a}C_{H0}u_{\rm a}\alpha'[q_{\rm sat}(T_{\rm g}) - q_{\rm a}]\,, \tag{18a}$$

$$H_{\rm sh} = H_{\rm sg} = \rho_{\rm a}c_p C_{H0}u_{\rm a}(T_{\rm g} - T_{\rm a})\,, \tag{18b}$$

$$\alpha' = \min(1, w_{\rm g}/w_{\rm k})\,, \tag{18c}$$

where $\rho_{\rm a}$ is the density of dry air. C_{H0} is the bare ground moisture or heat transfer coefficient.

However, if the ground is covered by vegetation, then the formulae for H and E need to be modified. We use $C_{H{\rm g}}$ as the ground moisture or heat transfer coefficient, and $C_{H{\rm h}}$ as the moisture or heat transfer coefficient on the dense canopy. So the value of $C_{H{\rm g}}$ ranges from C_{H0} to $C_{H{\rm h}}$, and the specific relation can be given by

$$C_{H{\rm g}} = (1-\sigma_{\rm f})C_{H0} + \sigma_{\rm f}C_{H{\rm h}}\,. \tag{19}$$

Within the canopy, the mean wind which both ventilates the foliage and promotes weak heat and moisture fluxes from the ground surface are denoted as $u_{\rm af}$ and prescribed by

$$u_{\rm af} = 0.83\sigma_{\rm f}C_{H{\rm h}}^{1/2}u_{\rm a} + (1-\sigma_{\rm f})u_{\rm a}\,. \tag{20}$$

Analogously, we define $T_{\rm af}$ and $q_{\rm af}$ to describe the properties within the canopy, and their expressions are listed as

$$T_{\rm af} = (1-\sigma_{\rm f})T_{\rm a} + \sigma_{\rm f}(0.3T_{\rm a} + 0.6T_{\rm f} + 0.1T_{\rm g}) \,, \quad (21a)$$

$$q_{\rm af} = (1-\sigma_{\rm f})q_{\rm a} + \sigma_{\rm f}(0.3q_{\rm a} + 0.6q_{\rm f} + 0.1q_{\rm g}) \,. \quad (21b)$$

Formulae (21a) and (21b) prescribe $T_{\rm af}$ and $q_{\rm af}$ to be the same as $T_{\rm a}$ and $q_{\rm a}$, respectively, in the absence of foliage. With these definitions, H can be calculated from

$$H_{\rm sf} = 1.1 I_{\rm LA} \cdot \rho_{\rm a} c_p C_{\rm f} u_{\rm af}(T_{\rm f} - T_{\rm af}) \,. \quad (22)$$

The evaporation rate per unit area from a representative leaf $E_{\rm leaf}$ is

$$E_{\rm leaf} = \rho_{\rm a} C_{\rm f} u_{\rm af}[q_{\rm sat}(T_{\rm f}) - q_{\rm af}]r'' \,. \quad (23)$$

The net foliage evaporation rate per unit horizontal ground area, $E_{\rm f}$, is

$$E_{\rm f} = I_{\rm LA} \cdot E_{\rm leaf} = I_{\rm LA} \cdot \rho_{\rm a} C_{\rm f} u_{\rm af}[q_{\rm sat}(T_{\rm f}) - q_{\rm af}]r'' = r''(E_{\rm f})_{\rm pot} \,. \quad (24)$$

After figuring out latent and sensible heat from the foliage surface, we still need to get their values on the ground (not bare):

$$H_{\rm sg} = \rho_{\rm a} c_p C_{Hg} u_{\rm af}(T_{\rm g} - T_{\rm af}) \,, \quad (25)$$

$$E_{\rm g} = \rho_{\rm a} C_{Hg} u_{\rm af}(q_{\rm g} - q_{\rm af}) \,. \quad (26)$$

So the total sensible heat flux $H_{\rm sh} = H_{\rm sf} + H_{\rm sg}$ is given by (22) and (25):

$$H_{\rm sh} = 1.1 I_{\rm LA} \cdot \rho_{\rm a} c_p C_{\rm f} u_{\rm af}(T_{\rm f} - T_{\rm af}) + \rho_{\rm a} c_p C_{Hg} u_{\rm af}(T_{\rm g} - T_{\rm af}) \,, \quad (27)$$

and $E_{\rm h} = E_{\rm f} + E_{\rm g}$ can be given by (24) and (26):

$$E_{\rm h} = I_{\rm LA} \cdot \rho_{\rm a} C_{\rm f} u_{\rm af}[q_{\rm sat}(T_{\rm f}) - q_{\rm af}]r'' + \rho_{\rm a} C_{Hg} u_{\rm af}(q_{\rm g} - q_{\rm af}) \,. \quad (28)$$

All the symbols in the equations from (22) to (28) are explained in the appendix, and their expressions are defined by Deardorff (1978).

By now, we have finished the parameterization of radiation flux and heat flux in Eq. (10). With the movement of the sun, all the values of those fluxes are changing, which causes the variation of $T_{\rm g}$ and $T_{\rm f}$. We need to use the value of $T_{\rm f}$ to calculate $H_{\rm sh}$ and $E_{\rm h}$ as showed above, which can be obtained from Eq. (15). However, before we can go on with our discussion, we must know the expression for $T_{\rm g}$ which is also a factor in (15). To solve the problem, we need to define another variable, T_2, which denotes the average temperature of ground in one day. Then we use the force restore method to get their values:

$$\frac{\partial T_{\rm g}}{\partial t} = \frac{c_1 G}{\rho_{\rm s} C_{\rm s} d_1} - \frac{c_2(T_{\rm g} - T_2)}{\tau} \,, \quad (29a)$$

$$\frac{\partial T_2}{\partial t} = \frac{G}{\rho_{\rm s} C_{\rm s} d_2} \,, \quad (29b)$$

where G is the soil heat flux obtained from Eq. (17). With the parameterization method proposed by Deardorff (1978), we can figure out $T_{\rm g}$ and T_2, and then all the other variables will be obtained.

2.3.2 *Variation of water content in and above the soil*

In the previous section, we discussed the energy balance between the land surface and atmosphere. The following text intends to solve some remaining problems in the process of parameterization. Our attention is focused on the soil water content $w_{\rm g}$ and w_2, and the volume of water remaining on the foliage, $W_{\rm dew}$, when it is raining.

We also need to take into consideration the transpiration when plants absorb solar rays, and the rate of transpiration is given by

$$E_{\rm tr} = \delta_{\rm c}(E_{\rm f})_{\rm pot}[r_a/(r_{\rm s}+r_{\rm a})] \times [1-(W_{\rm dew}/W_{\rm dew,\ max})^{2/3}] \,. \quad (30)$$

Then we can obtain w_2 and $w_{\rm g}$ by

$$\frac{\partial w_{\rm g}}{\partial t} = \frac{-C_1(E_{\rm g} + 0.1E_{\rm tr} - P_{\rm g})}{\rho_{\rm w} d_1'} - \frac{C_2(w_{\rm g} - w_2)}{\tau} \,, \quad (31a)$$

$$\frac{\partial w_2}{\partial t} = -\frac{E_{\rm g} + E_{\rm tr} - P_{\rm g}}{\rho_{\rm w} d_2'} \,, \quad (31b)$$

where $P_{\rm g}$ represents precipitation. C_1 and C_2 are empirical constants, whose expressions can be found in Deardorff's paper (1978).

The foliage surface specific humidity $q_{\rm f}$ needed in (21b) is obtained from

$$q_{\rm f} = r'' q_{\rm sat}(T_{\rm f}) + (1-r'')q_{\rm af} \quad (32a)$$

with restriction

$$q_{\rm f} \leqslant q_{\rm sat}(T_{\rm f}) \,. \quad (32b)$$

And $q_{\rm g}$ is given by

$$q_{\rm g} = \alpha' q_{\rm sat}(T_{\rm g}) + (1-\alpha')q_{\rm af} \,, \quad (33a)$$

where

$$\alpha' = \min(1, w_{\rm g}/w_{\rm k}) \quad (33b)$$

also with restriction

$$q_{\rm g} \leqslant q_{\rm sat}(T_{\rm g}) \,. \quad (33c)$$

The above expression (33) for $q_{\rm g}$ is given by Deardorff (1978). However, when it was used, we found that the value of the specific humidity of the desert

surface became unusually high, so this way of parameterization might not be suitable for bare ground. To solve the problem, we use the method proposed by Noilhan and Planton (1989), as

$$q_{\rm g} = R_{\rm hu} \cdot q_{\rm sat}(T_{\rm g}) \,, \tag{34}$$

where $R_{\rm hu}$ is the relative humidity at the ground surface, whose value is related to the superficial soil moisture $w_{\rm g}$.

$$R_{\rm hu} = \begin{cases} \dfrac{1}{2}\left[1 - \cos\left(\dfrac{w_{\rm g}}{w_{\rm k}}\pi\right)\right] & w_{\rm g} < w_{\rm k} \,, \\ 1.0 & w_{\rm g} \geqslant w_{\rm k} \,. \end{cases} \tag{35}$$

With this improvement, the numerical simulations obtain reasonable results.

3. Difference scheme and initial and boundary conditions

3.1 *Difference scheme and computation domain*

In the model, the forward upstream difference scheme is adopted for the time difference. Most of the calculations utilize a second-order spline difference, except for the advection terms, which adopt a third-order spline difference. The time step is 10 s. All the times appearing in this paper are local times. When programming, Eqs. (1)–(3) can be broken up into two main parts, which are written as

$$\frac{\partial \phi}{\partial t} = A_\phi + F_\phi \,,$$

where A_ϕ is the advection term and F_ϕ is the turbulence term

$$A_\phi = -u\frac{\partial \phi}{\partial x} - w\frac{\partial \phi}{\partial z} \,,$$

and

$$F_\phi = K_H \frac{\partial^2 \phi}{\partial x^2} + \frac{\partial}{\partial z}\left(K_\phi \frac{\partial \phi}{\partial z}\right) \,.$$

As for the spatial difference, we need first to set up a grid, which is made up of 30×21 points with 30 in the horizontal direction and 21 in the vertical direction. Each point records the state of the surrounding atmosphere. The horizontal grid spacing is 1000 m, with the first 15 kilometers representing desert and the others representing oasis, whose vegetation fraction is set to 0.75 in the model. In the vertical direction, the grids' heights are set as (m): 0, 2, 10, 20, 50, 80, 100, 150, 200, 250, 300, 400, 500, 750, 1000, 1250, 1500, 2000, 2500, 3000, 4000, and reference height $z_{\rm a} = 2$ m.

3.2 *Initial and boundary conditions*

The initial velocity profiles (m s^{-1}, where the minus sign represents an east wind) are

$$u(i,k) = \begin{cases} -4.5\left(\dfrac{z}{10}\right)^{0.14} & z \leqslant 1500 \text{ m} \,, \\ u|_{z=1500\text{ m}} & z > 1500 \text{ m} \,. \end{cases}$$

The initial potential temperature profiles (K) are

$$\theta(i,k) = \begin{cases} 298.0 & z \leqslant 1000 \text{ m} \,, \\ 298.0 + \dfrac{1.5(z-1000)}{100} & 1000 \text{ m} < z \leqslant 1500 \text{ m} \,, \\ 305.5 + \dfrac{0.5(z-1500)}{100} & z > 1500 \text{ m} \,. \end{cases}$$

The initial specific humidity profiles are shown in Table 1.

The initial turbulence kinetic energy, (m^2 s^{-2}) is

$$e^2(i,k) = \begin{cases} 0.1 & z \leqslant 1000 \text{ m} \,, \\ 0.05 & 1000 \text{ m} < z \leqslant 1500 \text{ m} \,, \\ 0.01 & z > 1500 \text{ m} \,. \end{cases}$$

The initial average temperature of a day (K) is

$$T_2(i) = 282.0 \,.$$

The initial water content of the soil (m m^{-1}) is

Desert: $w_{\rm g} = 0.05 \,, \quad w_2 = 0.15 \,;$

Oasis: $w_{\rm g} = 0.20 \,, \quad w_2 = 0.25 \,;$

$w_{\rm k} = 0.30 \,, \quad w_{\rm max} = 1.33 w_{\rm k} \,, \quad w_{\rm wilt} = 0.10 \,.$

The initial interception of precipitation (kg m^{-2}) is

$$W_{\rm dew} = 0.0 \text{ and } W_{\rm dmax} = \sigma_{\rm f} \,.$$

Table 1. The initial specific humidity profiles.

Desert		Oasis	
z (m)	q g kg^{-1}	z (m)	q g kg^{-1}
0	5.5	0	8.5
2	5.0	2	8.0
10	4.5	10	7.5
20	4.3	20	7.3
50	4.0	50	7.0
80	3.7	80	6.7
100	3.5	100	6.5
150	3.4	150	6.3
200	3.2	200	6.2
250	3.0	250	6.0
300	2.9	300	5.9
400	2.8	400	5.6
500	2.7	500	5.4
750	2.5	750	5.2
1000	2.3	1000	5.0
1250	2.0	1250	4.1
1500	1.6	1500	3.5
2000	1.4	2000	2.5
2500	1.2	2500	1.6
3000	1.0	3000	1.0
4000	0.5	4000	0.6

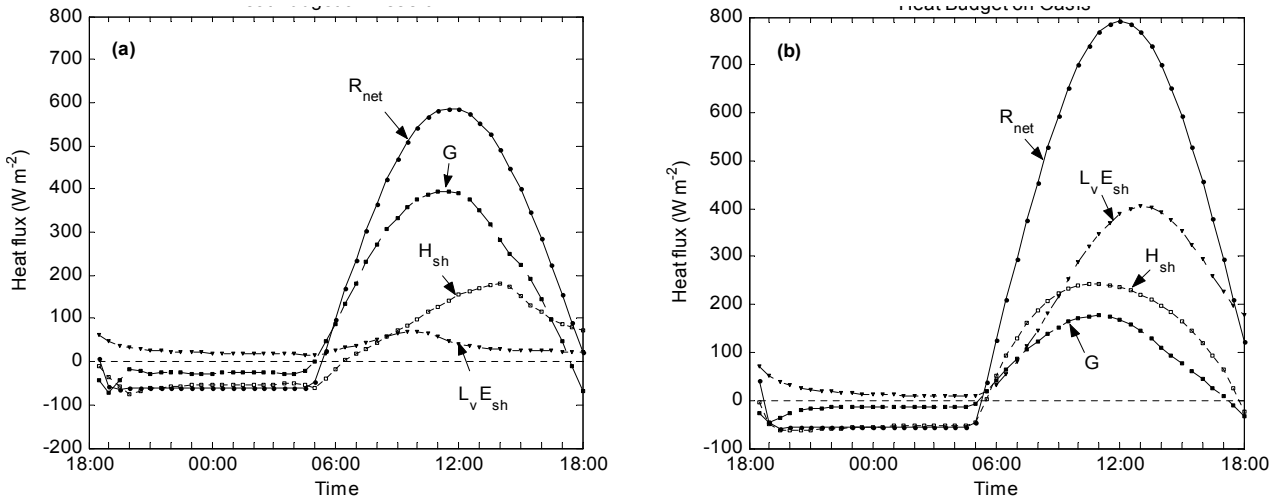

Fig. 1. Variation of heat flux on the land surface over a one-day period: (a) Dessert, (b) Oasis.

The boundary conditions at the top of the model are

$$z = 4000 \text{ m}, \quad \pi = 840 \text{ J kg}^{-1}\text{K}^{-1}.$$

The boundary conditions at the bottom of the model are

$$u(i,1) = 0 \text{ m s}^{-1} .$$

The boundary conditions on the left side of the grids are

$$w(1,k) = w(2,k) , \quad \theta(1,k) = \theta(2,k) .$$

The boundary conditions on the right side of the grids are

$$w(30,k) = w(29,k) , \quad \theta(30,k) = \theta(29,k) .$$

4. Results and analyses

4.1 *Circulations and interrelations between desert and oasis*

The topic listed above is the central problem we will discuss in this paper. Because of the difference in the properties of the ground surface, different physical processes may take place with the same external force like radiation, rainfall, and so on. Our model is based on a region that is divided equally into desert and oasis, so the correlation between them becomes the most important subject of our interest. The fraction of vegetation in the oasis in our model is set to 0.75.

First of all, we take a look at the energy budgets in the desert and oasis respectively. Figure 1 shows their difference. R_{net} represents the net radiation received by the ground, including the part covered by plants. Its expression is

$$R_{\text{net}} = S_{\text{h}}^{\downarrow} - S_{\text{h}}^{\uparrow} + R_{\text{Lh}}^{\downarrow} - R_{\text{Lh}}^{\uparrow} ,$$

where all the symbols in the equation are explained in the introduction of the numerical model. G is land flux, which is negative when passing upwards and positive when downwards. H_{sh} is sensible heat flux and $L_{\text{v}}E_{\text{sh}}$ is latent heat flux. Compared with desert, oasis receives more net radiation than desert does. That is because the ground surface temperature in oasis is much lower than that in the desert, which causes the value of $R_{\text{Lh}}^{\uparrow}$ in oasis to be less than that in the desert. Energy received by bare ground is consumed mostly in two ways: transfer into deep soil (G) or emission into air (H_{sh}), while the water latent heat is very little in the dry desert. On the other side, loss of energy in the form of latent heat flux plays a chief role in oasis. Pay attention to the sequence of peaks of sensible heat flux and latent heat flux in panel (b). As it shows, H_{sh} reaches its maximum value at around 11:00, and afterwards it decreases gradually. At the same time, $L_{\text{v}}E_{\text{sh}}$ becomes larger and larger and arrives at its peak at about 13:00. The reason for the phenomenon is that the ground temperature rises quickly after the sun rises, which causes H_{sh} to increase quickly. So H_{sh} reaches its maximum before noon. As the land surface becomes hotter, the water in the soil loses a great deal of mass in the form of vapor, which makes the soil drier. Then the roots of the plants will draw water from deeper soil, and as a result, latent heat increases and sensible heat decreases. However, as the atmosphere gets hotter and hotter, the stomata of plants will be closed to protect the vegetation from dehydration, causing the transpiration rate to fall.

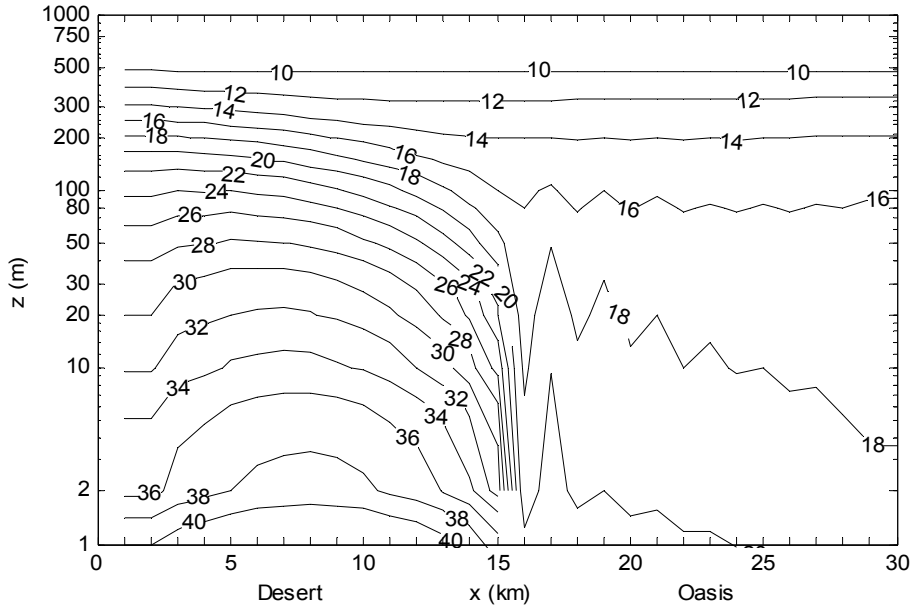

Fig. 2. Spatial distribution of predicted temperature (K) at 14:00.

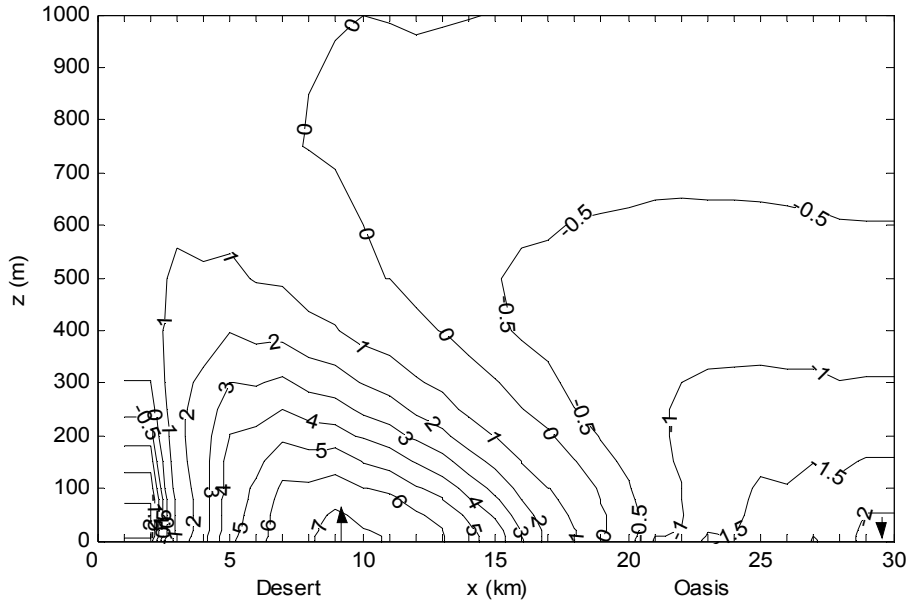

Fig. 3. Contours of vertical velocity w (cm s^{-1}) above the desert and oasis at 16:00.

The difference between the energy budgets of the desert and the oasis leads to the special temperature distribution shown in Fig. 2. It can be clearly seen that below 500 m, the air temperature over the desert is higher than that over the oasis at the same altitude. Su and Hu (1987) observed this phenomenon and called it the 'cold island effect', which is a figurative way to describe the oasis as a source of cool air. In Fig. 2, we can also see the fluctuation of the temperature above the oasis, which is the result of the heat wave from the hot desert.

As we know, the density of hot air is lower than that of cool air, so this structure of temperature will surely lead to the movement of air between oasis and

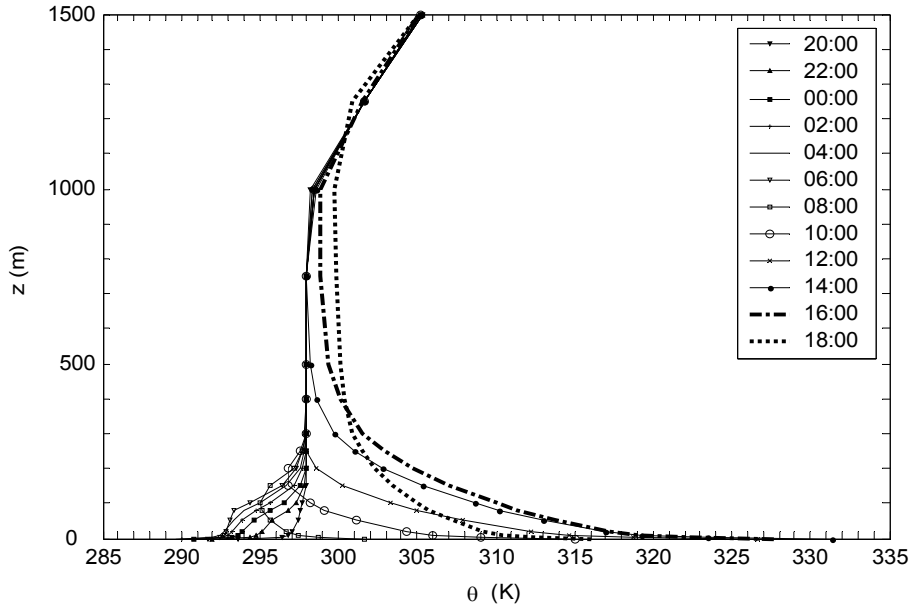

Fig. 4. Variation of the profile of potential temperature over the desert.

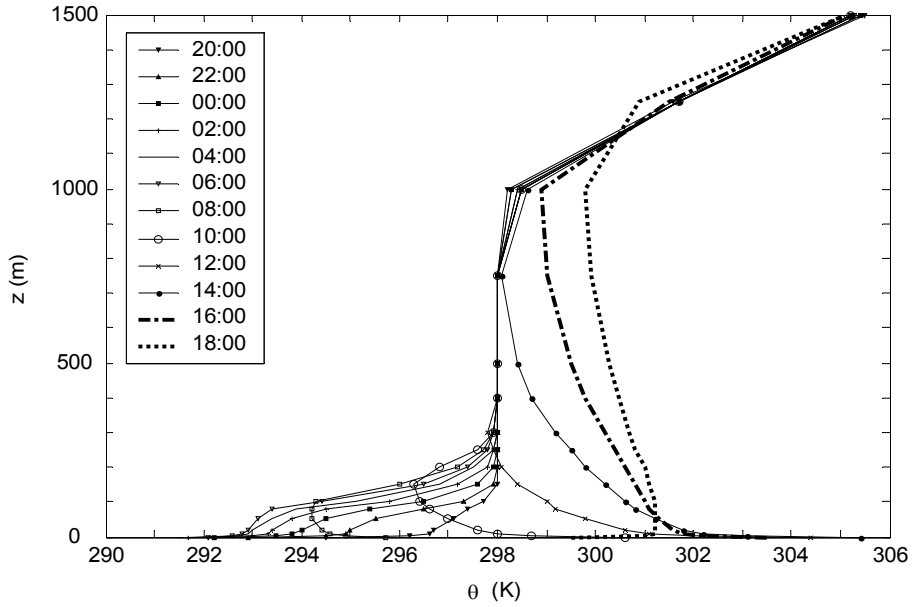

Fig. 5. Variation of the profile of potential temperature over the oasis.

desert. Using the data of the vertical velocity at 16:00 when such movement is the most intense, we draw Fig. 3. The contours show the situation we have discussed above. The direction of the arrows indicates the direction of w. They indicate that there is a center of updraft near the surface of the desert, which is consistent with the hottest place shown in Fig. 2. Results of the simulation have been corroborated by the calculations conducted by Miao and Ji (1993). Because the potential temperature profile at that time is superadiabatic, the heat flux is positive (upwards) over the desert and negative (downwards) over the oasis (Stull, 1991). As a result, a circulation of heat between the desert and oasis is set up.

By now we have discussed the potential temperature profiles, so then let us look at the result calculated by the computer. Figures 4 and 5 are drawn for such a purpose. Both the profiles of the desert and of the

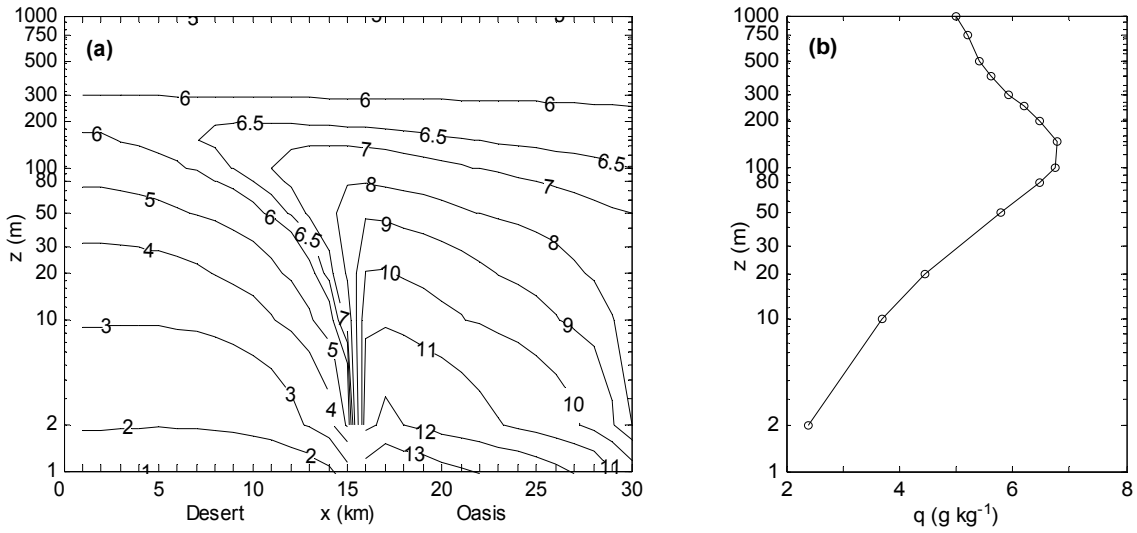

Fig. 6. (a) Spatial distribution of specific humidity at 12:00, (b) The profile of specific humidity over a point in the desert which is close to the oasis.

oasis are the most typical ones in the boundary layer. When the sun rises, the temperature of the ground becomes higher and higher, until it is much greater than the mean value at the adiabatic state and reaches the super-adiabatic unstable state during most of the daytime. But after sunset, the longwave radiation becomes the biggest part in the energy budget equation and causes a cooling effect on the land. As a result, the profiles become non-adiabatic, or become what is called temperature inversion.

There is another inversion that takes place in the daytime. Figure 6a shows the contours of the specific humidity distribution in space at 12:00. It is clearly seen that the air over the oasis is much wetter than that over the desert at the same height, which makes the oasis a wet island: a source of water vapor. Another interesting phenomenon is contained in this figure: a moisture tongue extending from oasis to the desert at heights from 2 m to 200 m. As a result, the moisture in the upper atmosphere is even moister than that in the lower height, bringing about a moisture inversion as showed in the profile of humidity based on a point at 10 km (Fig. 6b). This moisture inversion has been observed by Hu et al (1993) and also well simulated by Liu et al (1997).

At the end of this part, we will discuss the energy of turbulence, which is the typical phenomenon in boundary layer. Figure 7 utilizes data at 16:00. It shows that there is a center of turbulence kinetic energy, where the movement of the atmosphere is quite intense. On the other hand, the air over the oasis is relatively quiet, indicating the stability provided by vegetation.

Figure 8 reveals the same conclusion by showing the distribution of K_z in space. The picture tells us that there are two centers in the upper atmosphere, one is over the desert and the other is over the oasis. However, the value of the former is higher than that of the for the same reason we have discussed. The validation of this simulation result has been proved by Su and Hu (1987).

4.2 *Wind field analyses*

This part is a helpful supplement for the previous topic. By now, we have discussed several processes taking place above the desert and the oasis, together with the variation of physical variables. However, we ignored the wind field between them. As the most direct form, the change of the wind field reflects how deep their interaction is, and its development reveals the commencement, evolution and dying out of all the physical processes.

Figure 9 shows the diurnal variation of wind field during a day calculated by the model. We can see that the atmosphere is still quite stable and uniform in the morning, with little updraft and downdraft. This is because of the restraint of the SBL (stable boundary layer), which forms at night. After the sun rises, the ground surface becomes heated, causing the surrounding air to be hot. As a result, some small waves appear within atmosphere. Besides, according to thermodynamics, the SBL gradually changes into the ML (mixed layer), whose thickness becomes larger and larger with time. However, because of the limit of heating, there is not much conspicuous change in the figure from 6:00 to 10:00. When it reaches 12:00, the time when the

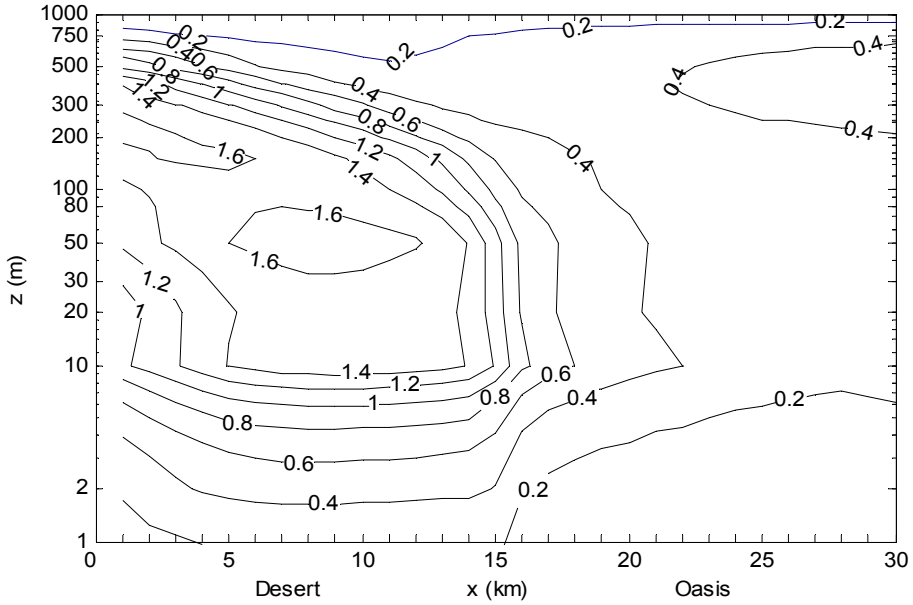

Fig. 7. Spatial distribution of turbulence kinetic energy e^2 ($m^2\ s^{-2}$) at 16:00.

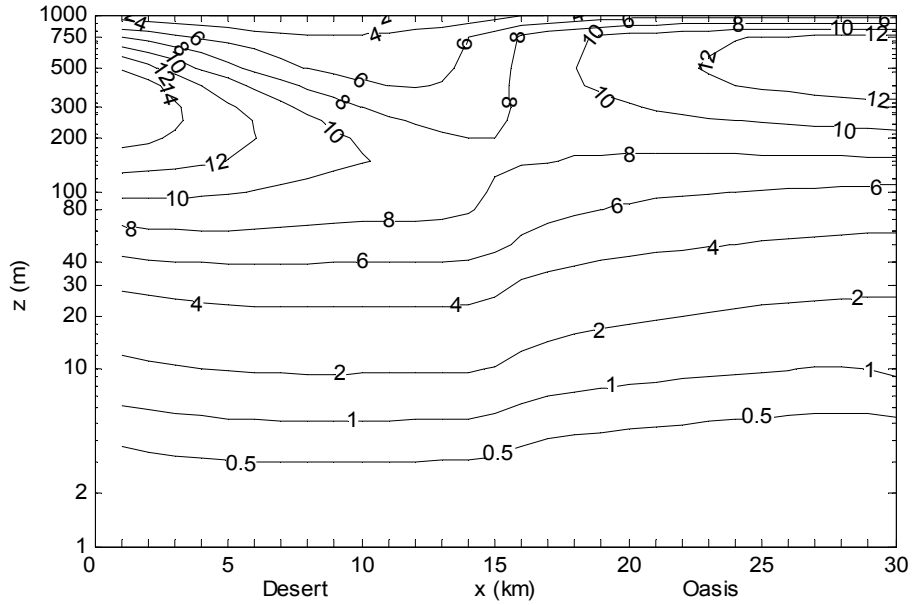

Fig. 8. Spatial distribution of turbulence exchange coefficient K_m at 16:00.

radiation from the sun arrives at its peak, the temperature of the land surface increases quickly and the movement of air becomes more active. From Figs. 9e, 9f, and 9g, we can see that there are violent updraft above desert and downdraft above oasis. You maybe be surprise that there is no circulation formed as predicted, that is because the initial wind field we set and the form of momentum equation we have chosen for simulation refrain us from getting the circulation (see 4.3). Comparing the updrafts and downdrafts, we can find that the former are somewhat more intense than the latter, which indicates that the air above the desert is more active than that above the oasis. Panel Fig. 9h shows that atmosphere becomes quite again, and we can guess that this kind of situation will maintain through the whole night, until a new day comes.

4.3 *Nocturnal boundary layer*

We have discussed the interactions between the

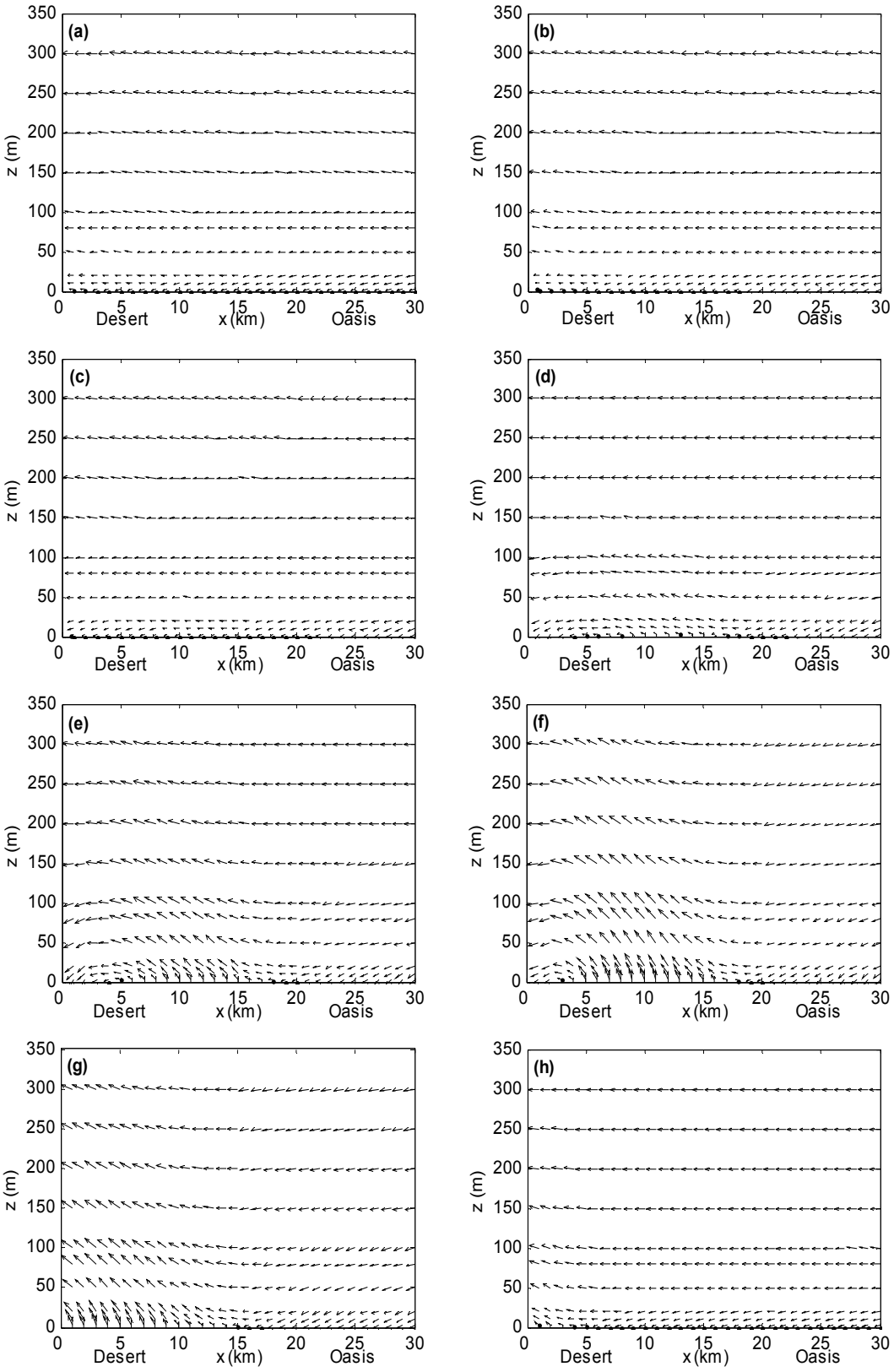

Fig. 9. Wind fields from 06:00 to 20:00 with an interval of 2 hours. (u: w=1 m s^{-1}: 1 cm s^{-1}) (a) 06:00, (b) 08:00, (c) 10:00, (d) 12:00, (e) 14:00, (f) 16:00, (g) 18:00, (h) 20:00.

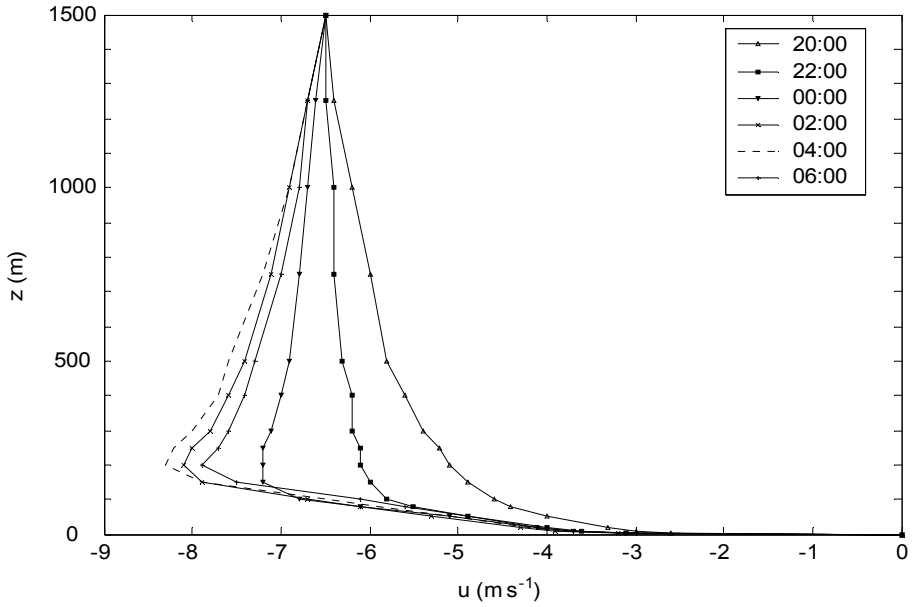

Fig. 10. Variation of the nocturnal wind profiles.

desert and the oasis, and now we will find out what happens at night. Here, we will neglect the radiative-cooling effect, which is the most important factor in the variation of the nocturnal ground surface temperature, and we will still obtain reasonable results. However, we need to make some modifications to the momentum equation by adding to the Coriolis terms:

$$\frac{\partial u}{\partial t} = -u\frac{\partial u}{\partial x} - w\frac{\partial u}{\partial z} + f_{\rm c}(v - v_{\rm g}) + K_{\rm H}\frac{\partial^2 u}{\partial x^2} + \frac{\partial}{\partial z}\left(K_{\rm z}\frac{\partial u}{\partial z}\right) , \tag{36a}$$

$$\frac{\partial v}{\partial t} = -u\frac{\partial v}{\partial x} - w\frac{\partial v}{\partial z} + f_{\rm c}(u_{\rm g} - u) + K_{\rm H}\frac{\partial^2 v}{\partial x^2} + \frac{\partial}{\partial z}\left(K_{\rm z}\frac{\partial v}{\partial z}\right) , \tag{36b}$$

where $f_{\rm c} = 1.45 \times 10^{-4} \sin\varphi$, and φ is the geographic latitude. According to the definition of geostrophic wind,

$$f_{\rm c} v_{\rm g} = \theta \frac{\partial \pi}{\partial x} .$$

This change is just for the sake of the numerical calculations, and it makes no difference to the theory.

After the transformation of the momentum equation, we still need to reset the initial conditions. In order to keep the uniformity, we will not change any of the previous values we have set, but just add some new ones:

$$u_{\rm g} = u|_{z=1500\ {\rm m}} , \quad v_{\rm g} = 0 .$$

Here, we set $v_{\rm g}$ to zero, and its effect is included in $u_{\rm g}$. As for the boundary conditions, we have:

$$u|_{z=0} = 0 , \quad v|_{z=0} = 0 .$$

The time step is still 10 s, and we just need to simulate this over a period of one day.

Figure 10 records the variation of the horizontal velocity profile at a point in the desert. As it shows, the wind is still a logarithmic velocity profile at 20:00. But after 22:00, the bottom of the curve becomes more and more extrusive. And the value of u is greater than $u_{\rm g}$ after 00:00. This common phenomenon at night is called the low altitude jet stream (Stull, 1991), which will be maintained through most of the night and reach its maximum at around 04:00, when the temperature of the ground surface is the lowest. Because K_z reflects how intense the air's motion is, its value will become larger and larger due to the great gradient of the wind. And this kind of trend is well showed in Fig. 11.

Figure 12 shows the spatial distribution of the predicted temperature at 04:00. We can see that most of the contours at night are horizontal and straight, which indicates that there is little movement in the air at night, except for some fluctuation near the ground. Besides, we can see that the temperature on the ground surface of the desert is lower than that of the oasis. This is because the land on the oasis is sheltered by green leaves, so that the loss of heat is less compared with that from the desert. As a result, the temperature of the oasis's surface is higher than that of the desert's, though the latter is much higher than

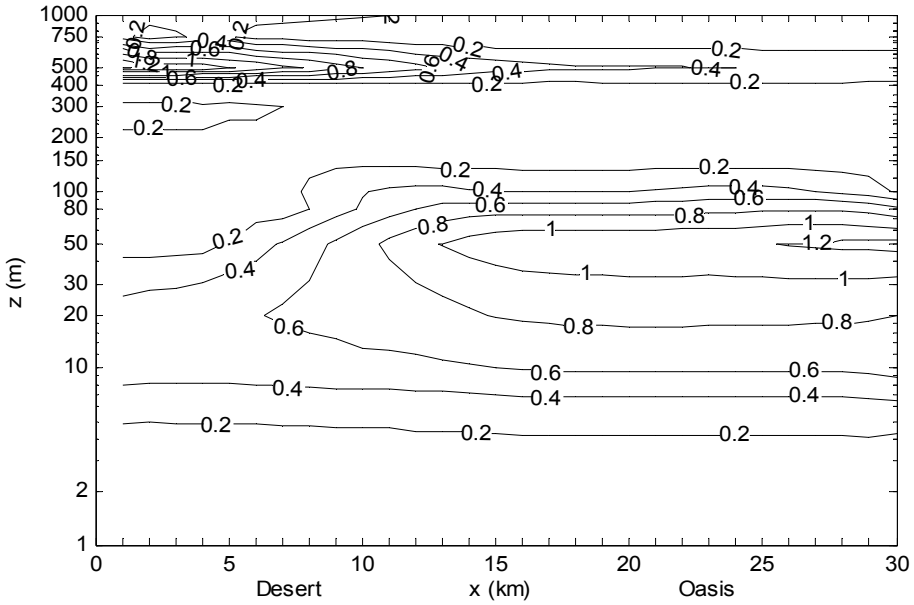

Fig. 11. Spatial distribution of turbulence exchange coefficient K_m at 04:00.

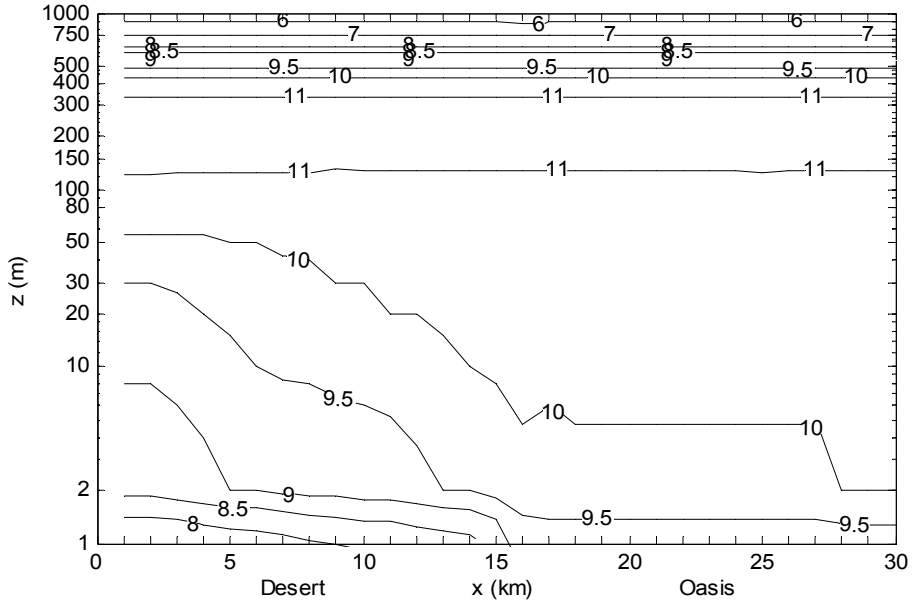

Fig. 12. Spatial distribution of predicted temperature (K) at 04:00

the former during the daytime.

5. Conclusions and discussions

A simple parameterization for a vegetation layer is developed and reasonable results are obtained, which is consistent with the observations of Su and Hu (1987) and Hu et al. (1993), and with the simulations of Liu et al. (2002, 1997) and Miao and Ji (1993). It is composed of equations of momentum, thermodynamics, water vapor, continuity, and static equilibrium, together with the energy-closed method in the solution of the turbulence parameterization. The model utilizes the most original way in the simulation of the land surface process proposed by Deardorff (1978). And the results show physical plausibility.

However, there are still some problems remaining with this method of simulation. For example, Figure 1 shows a rough relation in the energy budget. From the

curve, we can see that the value of G over the desert is unusually high. In addition, the parameterization is somewhat too simple, for example, in our model, $I_{\rm LA} = 7\sigma_{\rm f}$. The relationship between $I_{\rm LA}$ and $\sigma_{\rm f}$ is in fact very complicated in botany. The validation of some expressions for the parameters also needs to be tested by experiments.

Although there are some flaws, the model still gives some reasonable results as showed above. In our next paper, several sensitivity experiments are designed to test the stability and sensibility of this modified model.

Acknowledgments. This study was supported by the National Natural Science Foundation of China (Grant No. 40275004) and the State Key Laboratory of Atmosphere Physics and Chemistry, and the City University of Hong Kong (Grant No. 8780046) and the City University of Hong Kong Strategic Research (Grant No.7001038).

APPENDIX

List of Symbols

c_p specific heat capacity of dry air at constant pressure (1004 J kg^{-1} K^{-1})
C_{H0} bare ground moisture or heat transfer coefficient (0.0057)
$C_{H\rm h}$ the moisture or heat transfer coefficient on the dense canopy (0.0096)
$C_{H\rm g}$ ground moisture or heat transfer coefficient
$C_{\rm s}$ heat conductivity of soil ($\rho_{\rm s}C_{\rm s} = 1.554 \times 10^6$ J m^{-3} K^{-1})
e^2 turbulence kinetic energy (m^2 s^{-2})
$E_{\rm h}$ evapotranspiration rate (kg m^{-2} s^{-1})
$E_{\rm f}$ water evaporation rate from foliage (kg m^{-2} s^{-1})
$E_{\rm g}$ water evaporation rate at the ground (kg m^{-2} s^{-1})
g acceleration of gravity (m s^{-2})
$H_{\rm sh}$ total sensible heat flux (W m^{-2})
$H_{\rm sf}$ sensible heat flux from foliage (W m^{-2})
$H_{\rm sg}$ sensible heat flux from ground (W m^{-2})
K_H horizontal turbulence exchange coefficient (10.0 m^2 s^{-1})
K_m vertical turbulence exchange coefficient of momentum (m^2 s^{-1})
K_θ vertical turbulence exchange coefficient of heat (m^2 s^{-1})
K_q vertical turbulence exchange coefficient of humidity (m^2 s^{-1})
K_{e^2} vertical exchange coefficients of turbulence kinetic energy (m^2 s^{-1})
k von Kármán constant (0.4)
L master turbulence length scale
$L_{\rm v}$ latent heat of water vapor (2.5×10^6 J kg^{-1})
$I_{\rm LA}$ net leaf area index
p atmospheric pressure (hPa)
p_0 reference pressure (1000 hPa)
q specific humidity of the atmosphere (kg kg^{-1})
$q_{\rm a}$ specific humidity of the air at height z_a (kg kg^{-1})
$q_{\rm g}$ specific humidity of the ground (kg kg^{-1})
$q_{\rm f}$ specific humidity of the surface of foliage (kg kg^{-1})
$q_{\rm af}$ specific humidity of the atmosphere within the canopy (kg kg^{-1})
$R_{\rm net}$ net radiation received by the ground (W m^{-2})
S_0 solar constant (1367 W m^{-2} s^{-1})
t time (h)
T temperature of the atmosphere (K)
$T_{\rm a}$ temperature of the air at height $z_{\rm a}$ (K)
$T_{\rm g}$ temperature of the ground (K)
$T_{\rm f}$ temperature of the foliage surface (K)
$T_{\rm af}$ temperature of the atmosphere within the canopy (K)
u velocity of the atmosphere in the horizontal direction (m s^{-1})
$u_{\rm af}$ velocity of mean wind within the canopy (m s^{-1})
w velocity of the atmosphere in the vertical direction (m s^{-1})
$w_{\rm g}$ volume fraction of soil moisture on the ground (m m^{-1})
w_2 net volume fraction of soil moisture (m m^{-1})
$w_{\rm k}$ volume of water held by soil when the surface acts as if it were saturated (m m^{-1})
$w_{\rm max}$ maximum volume fraction of soil moisture (m m^{-1})
$w_{\rm wilt}$ water fraction when plants reach wilting point (m m^{-1})
$W_{\rm dew}$ interception of water on the foliage when raining (kg m^{-2})
$W_{\rm dew,\ max}$ maximum of $W_{\rm dew}$ (kg m^{-2})
$z_{\rm a}$ top of the canopy (2 m)
δ declination of the Sun (19°)
ω hour angle
τ time constant (86400 s)
$\sigma_{\rm f}$ vegetation fraction
$\sigma_{\rm c}$ cloud fraction
σ Boltzman constant (5.67×10^{-8} W m^{-2} K^{-4})
$\varepsilon_{\rm g}$ emissivity of the ground (0.95)
$\varepsilon_{\rm f}$ emissivity of foliage (0.95)
α attenuating ratio of shortwave radiation caused by atmosphere (0.15)
$\alpha_{\rm f}$ vegetable albedo (0.20)
$\alpha_{\rm g}$ albedo of the ground
φ geographical latitude (39°N)
θ atmospheric potential temperature (K)
λ a parameter of the soil property
$\rho_{\rm a}$ density of dry air (1.29 kg m^{-3})
$\rho_{\rm w}$ density of water (1000 kg m^{-3})
$\rho_{\rm s}$ density of soil (kg m^{-3})

REFERENCES

Bhumralkar, C. M., 1975: Numerical experiments on the computation of ground surface temperature in an atmospheric general circulation model. *J. Appl. Meteor.*, **14**, 1246–1258.

Blackadar, A. K., 1976: Modeling the Nocturnal Boundary Layer. *Proc. Third Symp. on Atmospheric Turbulence, Diffusion and Air Quality.* Boston, Amer. Meteor. Soc., 46–49.

Charney, J. G., W. Quirk, S. Chow, and J. Kornfield, 1977: A comparative study of the effects of albedo change on drought in semi-arid regions. *J. Atmos. Sci.,* **34**, 1366–1385.

Deardorff, J. W., 1978: Efficient prediction of ground surface temperature and moisture with inclusion of a layer of vegetation. *J. Geophys. Res.,* **83**, 1889–1903.

Dickinson, R. E., A. Henderson-Sellers, and P. J. Kennedy, 1993: Biosphere-Atmosphere Transfer Scheme (BATS) version 1e as coupled to the NCAR community climate model. NCAR Tech. Rop. NCAR/TN-387+STR, Boulder (Colorado), NCAR 72pp.

Dickinson, R. E., A. Henderson-Sellers, P. J. Kennedy, and M. F. Wilson, 1986: Biosphere-Atmosphere Transfer Scheme (BATS) for the NCAR community climate model. NCAR Tech. Rop. NCAR/TN-275+STR. Boulder (Colorado): NCAR, 69pp.

Hu Yinqiao, Wang Junqin, and Zuo Hongchao, 1993: Character of water vapor transportation in the surface layer over desert near oasis. *Plateau Meteor.,* **12**, 125–132. (in Chinese)

Liu Shikuo, and Liu Shida, 1991: *Atmospheric Dynamics.* Peking University Press, Beijing, 77pp. (in Chinese)

Liu Shuhua, Huang Zichen, and Liu Lichao, 1997: Numerical simulation of the influence of vegetation cover factor on boundary layer climate in semi-arid region. *Acta Meteorologica Sinica.*, **11**, 66–78.

Liu Shuhua, Wen Pinghui, Zhang Yunyan, Hong Zhongxiang, Hu Fei, and Liu Huizhi, 2002: Sensitivity tests of interaction between land surface physical process and atmospheric boundary layer. *Acta Meteorologica Sinica*, **16**, 451–469.

Mahfouf, J. F., E. Richard, and P. Mascart, 1987: The influence of soil and vegetation on the development of mesoscale circulations. *J. Climate Appl. Meteor.*, **26**, 1483–1495.

Miao Manqian, and Ji Jingjun, 1993: Numerical Simulation of the atmospheric Boundary Layer structure Around Oasis. *Scientia Atmospherica Sinica.* **17**, 77–86. (in Chinese)

Noilhan, J., and S. Planton, 1989: A simple parameterization of land surface processes for meteorological models. *Mon. Wea. Rev.,* **117**, 536–549.

Sang Jianguo, Wu Yidan, Liu Huizhi, Pan Naixian, Chen Jiayi, and Zhang Aichen, 1992: Numerical simulation of atmospheric boundary layer over inhomogeneous underlying surface. *Plateau Meteorology*, **11**(4), 400–410. (in Chinese)

Sellers, P. J., Y. Mintz., Y. C. Sud., and A. Dalcher, 1986: A simple biosphere model (SiB) for use within general circulation models. *J. Atmos. Sci.,* **43**, 505–531.

Sellers, P. J., and coauthors, 1996: A revised land surface parameterization (SiB2) for atmospheric GCMs. Part I: Model formulation. *J. Climate,* **9**, 676–705.

Stull, R. B., 1991: *An Introduction To Boundary Layer Meteorology.* Qingdao Oceanic University Press, Qingdao, 63pp. (in Chinese)

Su Congxian, and Hu Yinqiao, 1987, The structure of the oasis cold island in the planetary boundary layer. *Acta Meteorologica Sinica.* **45**, 322–328. (in Chinese)

Wang Yongsheng, 1987: *Atmospheric Physics.* Peking University Press, Beijing, 166pp. (in Chinese)

Yamada, T., 1983: Simulations of Nocturnal Drainage Flows by a q^2l Turbulence Closure Model. *J Atmos. Sci.*, **40,** 91–106.